Short communication

Hydrodeoxygenation kinetics of syringol, guaiacol and phenol over H-ZSM-5

Kavimonica Venkatesan[a,b], J.V. Jayarama Krishna[a,b], S. Anjana[a], Parasuraman Selvam[c,d,e], Ravikrishnan Vinu[a,b,c,*]

[a] Department of Chemical Engineering, Indian Institute of Technology-Madras, Chennai 600036, India
[b] National Centre for Combustion Research and Development, Indian Institute of Technology-Madras, Chennai 600036, India
[c] National Centre for Catalysis Research, Indian Institute of Technology-Madras, Chennai 600036, India
[d] Department of Chemistry, Indian Institute of Technology-Madras, Chennai 600036, India
[e] School of Chemical Engineering and Analytical Science, The University of Manchester, Manchester M13 9PL, United Kingdom

ARTICLE INFO

Keywords:
Phenol
Guaiacol
Syringol
Hydrodeoxygenation
Kinetics
H-ZSM-5

ABSTRACT

This study is focused on understanding the hydrodeoxygenation (HDO) kinetics of pyrolysates from lignin such as phenol, guaiacol and syringol over H-ZSM-5 catalyst. The major products from syringol were guaiacol, phenol, anisole, cresol, benzene, and toluene. A reaction network was proposed to capture the transformations of syringol in which the transformations of guaiacol and phenol were included. A kinetic model comprising nine reactions of seven species was developed. The simulated yields of a majority of the HDO products matched well with experiments in the temperature range of 350-500 °C, substantiating that the obtained rate parameters reasonably represent the HDO kinetics.

1. Introduction

It is mandatory to enhance the quality of pyrolysis bio-oil via catalytic hydrodeoxygenation (HDO), as the oxygenated functional groups in bio-oil impart undesirable properties like low heating value, high acidity, and poor storage stability. The reaction chemistry of catalytic HDO can be well understood by using bio-oil model compounds instead of whole bio-oil, which is a complex mixture of many organic compounds. Lignin-derived compounds like phenol and methoxy phenols form a major class of compounds in bio-oil, and these are the precursors for the formation of aromatic hydrocarbons in the upgraded bio-oil.

Zanuttini et al. [1] investigated the effect of acid site type, strength, and density on deoxygenation of cresol using Pt-loaded supports of varying acidities, and showed that high metal-to-acid ratio is required to form highly deoxygenated product like toluene. Zhu et al. [2] elucidated the role of metal and acidic support in HDO of anisole using Pt/H-beta catalyst. It was shown that Pt is responsible for sequential demethylation, HDO and hydrogenation reactions resulting in the formation of phenol, benzene, and cyclohexane. Brønsted acid sites in H-beta promote the formation of phenol, cresol and xylenol via transalkylation reaction. Pt loaded on H-beta exhibited dual function, and accelerated both methyl transfer and HDO reactions producing benzene, toluene and xylene. Lee et al. [3] studied the role of bifunctional metal catalyst (Pt/Rh/Pd/Ru) supported on acid matrices (Al$_2$O$_3$/SiO$_2$-

Al$_2$O$_3$/nitric acid treated carbon-black) for HDO of guaiacol. Several other catalysts like Pt/Al$_2$O$_3$, Pt/ZrO$_2$, Rh/ZrO$_2$, Pd/ZrO$_2$, Pt/TiO$_2$, Pt/SiO$_2$, Pt/CeO$_2$, Mo$_2$C, W$_2$C-supported on carbon nanofibre, and Na$_2$CO$_3$/Al$_2$O$_3$ have been investigated for the conversion of lignin-derived bio-oil compounds into aromatic hydrocarbons [4–7]. In recent years, metal supported on zeolites such as H-ZSM-5, H-Beta and H−Y are widely used to catalyze the HDO of phenolic compounds owing to their high acidity [8–10].

Generally, the cleavage of C$_{aryl}$–OH bond occurs via direct deoxygenation or direct hydrogenolysis [10–12]. Alternatively, hydrogenation of the aromatic ring leads to the formation of cyclohexanol as an intermediate, followed by rapid dehydration and further hydrogenation to form cyclohexene and cyclohexane, respectively. Ni-supported H-ZSM-5 favors the formation of benzene [11], while Pd and Pt-supported on H-Beta and H−Y leads to the formation of bicyclic compounds [10,12]. Therefore, in this study, H-ZSM-5 has been chosen as a model catalyst. Furthermore, to design novel catalysts, a fundamental knowledge on kinetics of HDO of pyrolysates is important. However, studies on mechanistic kinetics of HDO of lignin model compounds are scarce.

The main objective of this study is to investigate the catalytic HDO of three model compounds, viz., phenol, guaiacol and syringol, over H-ZSM-5 catalyst at different temperatures. The stability and reactivity of these phenolic compounds are determined by the number of methoxyl

Table 1
Properties of H-ZSM-5 catalyst.

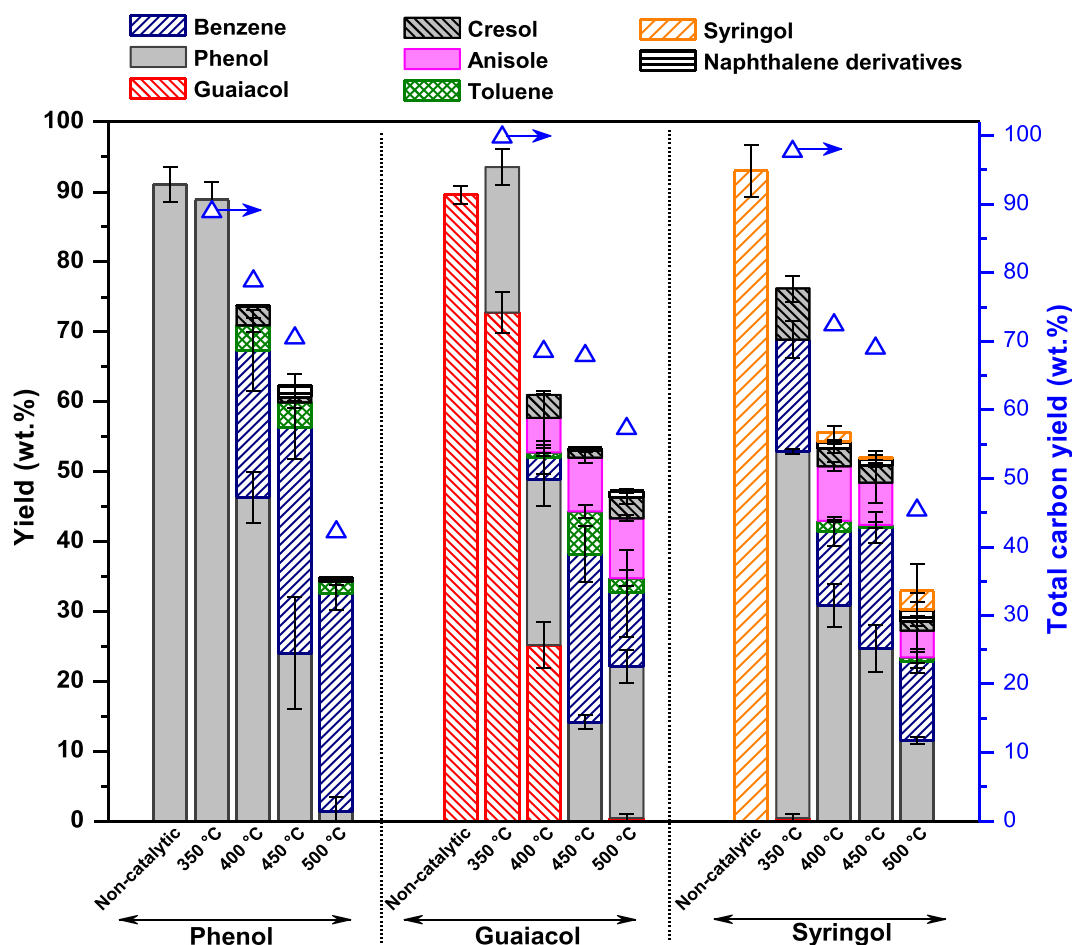| Surface acidity (mmol g^{-1})	Micropore area (m^2 g^{-1})	BET surface area (m^2 g^{-1})	Micropore volume (cm^3 g^{-1})	Average pore diameter (Å)
0.475	252	335	0.13	88.7

Fig. 1. Yields of HDO products from phenol, guaiacol and syringol using H-ZSM-5 catalyst maintained at different bed temperatures. The mass ratio of catalyst-to-model compound is 10:1. "Non-catalytic" corresponds to vaporization of phenol, guaiacol, and syringol at 190, 220 and 270 °C, respectively.

substitution in them. This study is the first of its kind to propose a mechanistic kinetic model to evaluate the rate parameters for the key steps, and validate the model yields of the major compounds with the experimental data at different temperatures.

2. Experimental section

2.1. Materials

Phenol, guaiacol and syringol (99% purity) were purchased from Alfa Aesar and were used as-received. Commercial ZSM-5 in ammonium form with Si/Al ratio of 50 was purchased from Alfa Aesar. The catalyst was converted to protonated form by calcining at 600 °C for 6 h with airflow of 30 mL min^{-1}. It was characterized by porosimetry and ammonia-temperature programmed desorption (NH$_3$-TPD) according to standard procedures reported elsewhere [13]. The catalyst properties are given in Table 1.

2.2. HDO experiments

Catalytic HDO experiments were performed in an analytical

pyrolyzer (Pyroprobe® 5200, C.D.S. Analytical, USA) integrated with a gas chromatograph/mass spectrometer (GC/MS) (Agilent 7890/5975, Agilent Technologies, USA). In a typical experiment, 0.2 ± 0.01 mg of the model compound was weighed accurately in a microbalance (Sartorius CUBIS series) and placed in the center of a 2 mm i.d. × 20 mm length quartz tube. The two ends of the quartz tube were packed using quartz wool to avert sample spillage, and it was inserted into the platinum coil probe, which was resistively heated at a ramp rate of 10,000 °C s^{-1}, and maintained at the set temperature for a hold time of 60 s. Phenol, guaiacol and syringol were vaporized at 190, 220, and 270 °C, respectively, and the vapors were carried by hydrogen gas (99.9995% purity) to the pre-heated catalyst bed. H-ZSM-5 catalyst was packed in a quartz tube (4 mm i.d. × 150 mm length) at a catalyst-to-sample ratio of 10:1 wt./wt. The HDO of model compounds was investigated at various catalyst bed temperatures, viz., 350, 400, 450, and 500 °C. The upgraded pyrolysis vapors were carried directly to the GC through the heated transfer line maintained at 250 °C. The GC injector was maintained at 300 °C with a split ratio of 200:1. The separation of pyrolysates was achieved in an Agilent HP-5 MS column (30 m length × 250 μm i.d. × 0.25 μm film thickness). The flow rate of helium gas (5.5 grade) through the column was 1.2 mL min^{-1}. The GC column
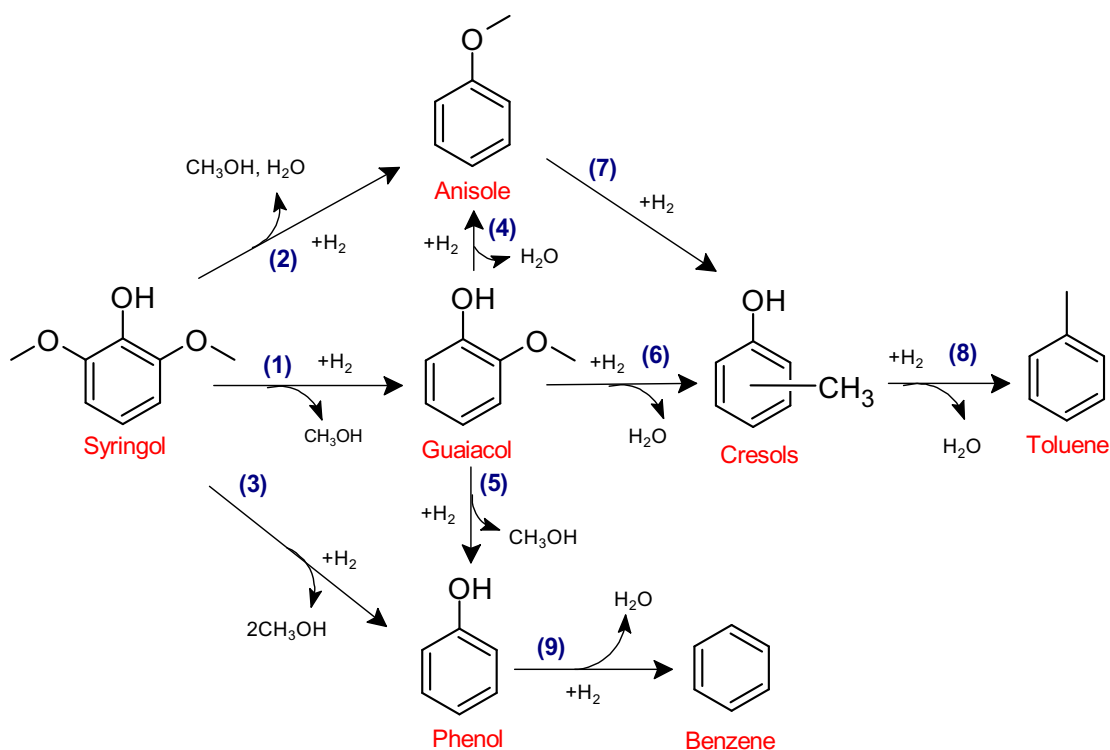
Fig. 2. Proposed reaction network for catalytic HDO of syringol.

oven was programmed as follows: 40 °C for 2 min, ramped at 30 °C min^{-1} to 280 °C, and finally held for 10 min at 280 °C. The GC/MS interface, MS ion source and quadrupole temperatures were maintained at 280, 250 and 150 °C, respectively. The electron ionization voltage in the MS was 70 eV. The mass-to-charge range scanned in the MS was 10–300 Da. The products were identified by comparing the mass spectra of the peaks in the GC total ion chromatogram with the NIST library of mass spectra. The major HDO products were identified with a match factor greater than 95%.

The model compounds and the major products, viz., syringol, guaiacol, phenol, benzene, toluene, anisole, and cresol, were calibrated in the GC using standards to calculate their wt% yields. It is important to note that low molecular weight compounds and gases including moisture, CO, CO$_2$, and CH$_3$OH could not be captured in the GC/MS. Using the quantified yields of the major compounds, carbon yield was also calculated to understand the mass balance closure. Owing to the low mass of the catalyst used (2 mg), the amount of coke deposited on the catalyst could not be captured accurately. All the experiments were repeated three times, and the reported yield data are average values with 4–8% standard deviation.

3. Results and discussion

3.1. Product analysis

Fig. 1 depicts the product yields from phenol, guaiacol and syringol at different catalyst bed temperatures. After vaporization, the quantified amounts of phenol, guaiacol and syringol were 91.0, 89.6 and 93.0 wt%, respectively. This shows that ≤10 wt% of the reactant was lost in experiments, and these values were used as the basis for investigating the deoxygenation extent of model compounds into HDO products over H-ZSM-5. With increase in temperature, the conversion of phenol increased in the following order: 350 °C (11.1%) < 400 °C (53.6%) < 450 °C (76.0%) < 500 °C (98.6%). The major product was benzene, which is formed by dehydration of phenol over the acidic sites of H-ZSM-5. In addition, minimal formation of cresol and toluene was

also observed. Fig. 1 also depicts the carbon balance achieved in the experiments. With increase in catalyst temperature, the yield of quantified products decreased due to the formation of gaseous products and coke on the catalyst surface, which were not quantified due to experimental limitations.

HDO of guaiacol is reported to proceed via three major routes [14]: (a) hydrogenolysis of the methoxy group to produce phenol, (b) hydrodeoxygenation of the hydroxyl group to form anisole, and (c) demethoxylation followed by subsequent acid-catalyzed methyl transfer reaction resulting in the formation of cresol. Moreover, the most favourable HDO pathway of guaiacol is demethoxylation of the methoxy group attached to the aromatic carbon, which results in the formation of phenol. This can be attributed to the low bond dissociation energy (BDE) of C$_{aryl}$–OCH$_3$ (102.9 kcal mol^{-1}) compared to C$_{aryl}$–OH (111.8 kcal mol^{-1}) in guaiacol [15]. The cleavage of C$_{aryl}$–OH bond in presence of hydrogen produces benzene at 400 °C. Two other proposed routes involving the formation of anisole and cresol also become prominent with increase in temperature. Cresol can also be formed by trans-alkylation of anisole [16,17]. Further increase in temperature to 450 °C led to hydrogenolysis of the hydroxyl group in cresol resulting in the formation of toluene. Apart from these major pathways, demethylation of methoxy group in guaiacol to produce catechol is reported as a possible route in several other studies using different catalysts [18,19]. However, due to the absence of catechol in the product spectrum, this pathway is not considered in this study. The conversion of guaiacol increased with increase in temperature, viz., 350 °C (27.3%) < 400 °C (74.8%). Beyond 400 °C, complete conversion of guaiacol was observed.

Unlike phenol and guaiacol, the behaviour of syringol is significantly different. Decomposition of syringol into various products was almost instantaneous with 100% conversion even at a low temperature of 350 °C. This is ascribed to its high reactivity induced by two methoxy groups. The two main HDO reactions involved in syringol include demethoxylation and dehydration. Direct deoxygenation of syringol produces guaiacol and phenol by the removal of one and two methoxy groups, respectively. Subsequently, guaiacol and phenol

Table 2
Kinetic parameters estimated for various reactions in the network presented in Fig. 2.

Reaction No.	A_i (s^{-1})	E_i (kJ mol^{-1})	k_i (s^{-1})			
			350 °C	400 °C	450 °C	500 °C
1	$(2.00 \pm 0.87) \times 10^5$	58.7 ± 3.0	2.39	5.56	11.48	21.60
2	$(2.30 \pm 0.75) \times 10^9$	151.0 ± 6.0	0.0005	0.0044	0.028	0.14
3	$(6.10 \pm 0.80) \times 10^6$	86.0 ± 2.6	0.375	1.29	3.73	9.40
4	$(3.00 \pm 1.50) \times 10^7$	104.3 ± 3.0	0.054	0.24	0.87	2.68
5	$(1.30 \pm 0.35) \times 10^6$	75.5 ± 2.0	0.610	1.79	4.56	10.28
6	$(1.75 \pm 1.30) \times 10^7$	100.6 ± 3.5	0.064	0.27	0.94	2.78
7	$(8.00 \pm 1.60) \times 10^7$	118.7 ± 5.7	0.009	0.049	0.21	0.76
8	$(1.75 \pm 0.90) \times 10^9$	124.0 ± 5.5	0.070	0.42	1.92	7.30
9	$(7.20 \pm 1.90) \times 10^6$	92.8 ± 1.5	0.120	0.45	1.42	3.86

undergo a series of reactions as described earlier. This is evident from the gradual decrease in the yield of phenol with temperature: 350 °C (52.4 wt%) > 400 °C (30.8 wt%) > 450 °C (24.7 wt%) > 500 °C (11.5 wt%). The major products at 350 °C from syringol include phenol, cresol, and benzene. Interestingly, no trace of guaiacol was observed in the products indicating its complete conversion. In addition, traces of naphthalene derivatives were also observed at certain experimental conditions. Notably, complete deoxygenation of phenol was not achieved when guaiacol and syringol were used as model compounds, which is due to the high stability of phenol. Based on the observed products, a reaction network has been proposed, which is depicted in Fig. 2.

3.2. Modeling framework

The following rate equations were developed for the multiple reaction network depicted in Fig. 2. As hydrogen is the reaction medium present at high concentration, all the reactions were assumed to be pseudo first order in the concentration of the phenolic compound.

$$\frac{dC_{syringol}}{d\tau} = -(k_1 + k_2 + k_3)C_{syringol} \tag{1}$$

$$\frac{dC_{guaiacol}}{d\tau} = k_1 C_{syringol} - (k_4 + k_5 + k_6)C_{guaiacol} \tag{2}$$

$$\frac{dC_{anisole}}{d\tau} = k_2 C_{syringol} + k_4 C_{guaiacol} - k_7 C_{anisole} \tag{3}$$

$$\frac{dC_{phenol}}{d\tau} = k_3 C_{syringol} + k_5 C_{guaiacol} - k_9 C_{phenol} \tag{4}$$

$$\frac{dC_{cresol}}{d\tau} = k_6 C_{guaiacol} + k_7 C_{anisole} - k_8 C_{cresol} \tag{5}$$

$$\frac{dC_{toluene}}{d\tau} = k_8 C_{cresol} \tag{6}$$

$$\frac{dC_{benzene}}{d\tau} = k_9 C_{phenol} \tag{7}$$

The rate constants, k_i, where $i = 1$ to 9, are assumed to be described by Arrhenius equation, given by, $k_i = A_i \exp(-E_i/RT)$, where A_i is the frequency factor and E_i is the activation energy of the elementary step. C_i is the species concentration and τ is the residence time of species (< 1 s). The objective function is defined as the sum of squares of the difference between the experimental yield and simulated yield obtained from the model.

$$S = \sum_{i=1}^{n_s} [(y)_{i,exp} - (y)_{i,cal}]^2 \tag{8}$$

For a particular set of parameters, the subscript i refers to the ith data point, n_s represents the total number of species considered, which are seven, and $(y)_{i,\ exp}$ and $(y)_{i,\ cal}$ refer to the experimental and

calculated yields, respectively. In this model, the number of unknown parameters to be determined are $2n_s$ (E_i, A_i, for $i = 1$ to n_s). The objective function corresponds to an optimization problem, which was solved using 'fmincon' sub-routine in MATLAB®. It is worthwhile to note that the experimental data correspond to the final yields of products. Therefore, the optimal values of the rate parameters correspond the best match of the product yields from the model with that of the experiments. Furthermore, the following rate equations were used to determine the simulated yields of water and methanol by using the optimized values of rate parameters.

$$\frac{dC_{H_2O}}{d\tau} = k_2 C_{syringol} + (k_4 + k_6)C_{guaiacol} + k_8 C_{cresol} + k_9 C_{phenol} \tag{9}$$

$$\frac{dC_{CH_3OH}}{d\tau} = (k_1 + k_2 + 2k_3)C_{syringol} + k_5 C_{guaiacol} \tag{10}$$

It is worthwhile to note that the HDO of phenol forms a subset of HDO of guaiacol, which then is a subset of HDO mechanism of syringol. Thus, the rate parameters of reaction (9) were initially estimated by executing the model for HDO of phenol. The model was then executed for HDO of guaiacol by using the rate parameters of reaction (9) from phenol HDO simulations in order to estimate the rate parameters of reactions (4–8). Finally, using the rate parameters of reactions (4–9), which were estimated from HDO of phenol and guaiacol, the HDO kinetic model of syringol was executed, and the rate parameters of reactions (1–3) were determined.

3.3. Kinetic model validation

The optimized rate parameters, A_i and E_i, for each of the reactions in Fig. 2 are given in Table 2. The rate constants at different temperatures are also provided. Reasonable estimates of the error bars for frequency factor and activation energy are also presented in Table 2. The A_i and E_i vary in the range of 10^5–10^9 s^{-1} and 58–151 kJ mol^{-1}, respectively. It is observed that reactions (1) and (5) occur faster (58.7 and 75.5 kJ mol^{-1}), while reactions (2), (7) and (8) happen at relatively slower rates (151, 118.7, and 124 kJ mol^{-1}). The methoxy groups present in syringol and guaiacol can be easily cleaved leading to the formation of methanol. Reactions (2) and (8) involve removal of hydroxyl groups producing water as a by-product. Based on the rate parameter values, it can be understood that deoxygenation occurs more readily via reactions (1), (3) and (5) that result in high yields of phenol. Importantly, from the activation energy and rate constant values of reactions (1), (3) and (5), it is evident that syringol, with two methoxy groups, is the least stable, followed by guaiacol under HDO conditions. On the other hand, the removal of hydroxyl group is relatively more difficult resulting in low yields of anisole and toluene. Similar results were reported by Nimmanwudipong et al. [20] for guaiacol conversion catalyzed by Pt/γ-Al$_2$O$_3$ at high partial pressures of hydrogen. Reactions (1), (3), (4), (5), (6) and (9) are extremely sensitive to activation energy, which is reflected by the low standard deviation.
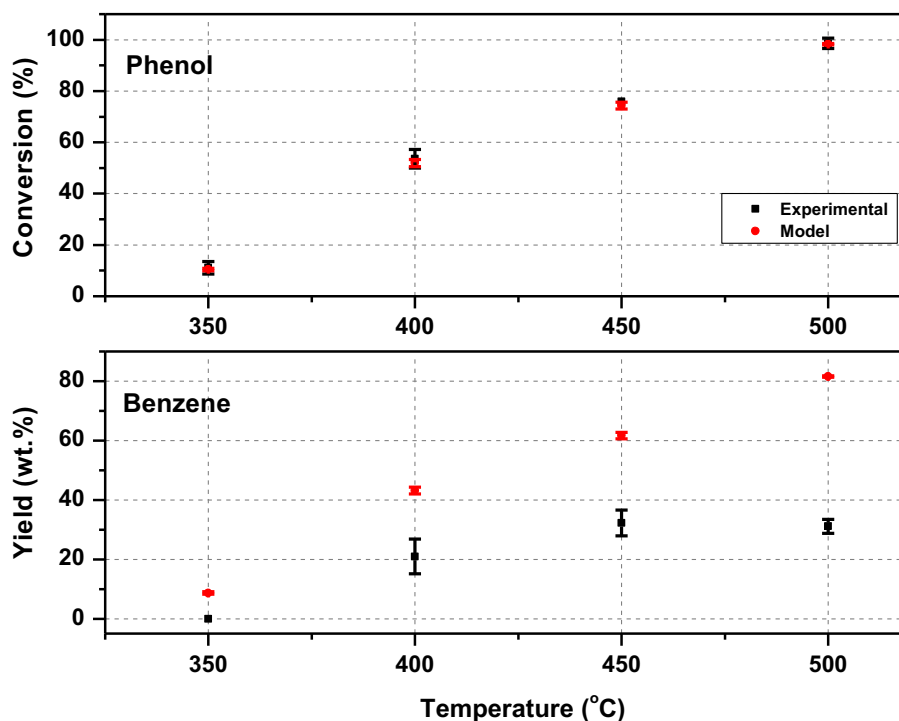
Fig. 3. Comparison of experimental and model yields of major products from catalytic HDO of phenol at different temperatures.
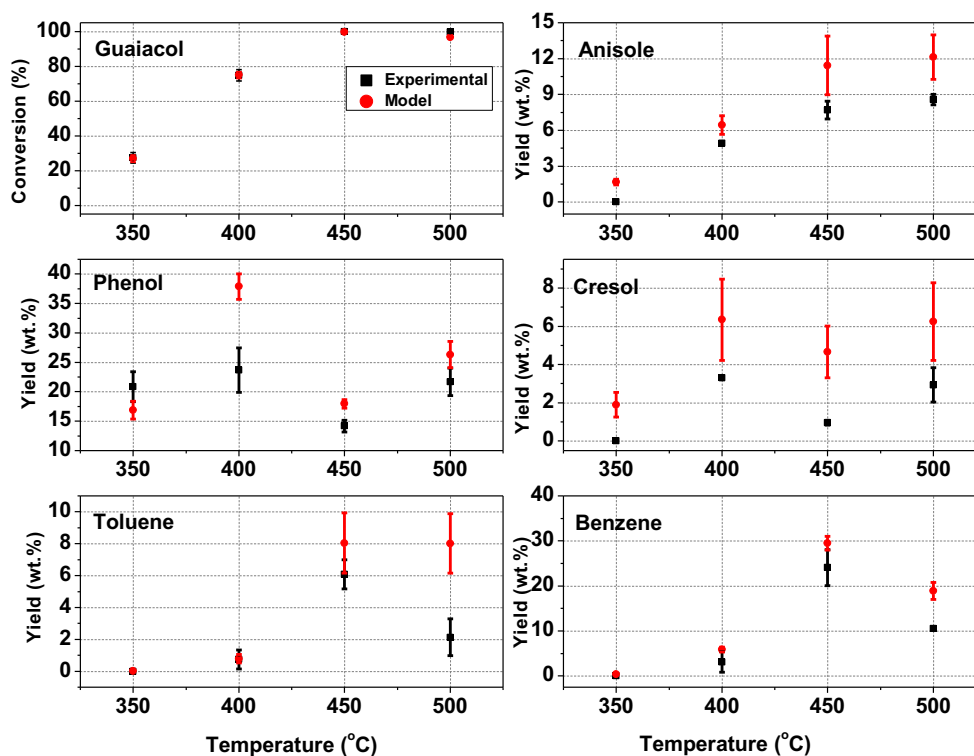

Fig. 4. Comparison of experimental and model yields of major products from catalytic HDO of guaiacol at different temperatures.

Figs. 3, 4 and 5 present a comparison of experimental and model yields of major products at different temperatures from catalytic HDO of phenol, guaiacol, and syringol, respectively. The error bars on the model yields are based on the standard deviation of rate parameters. It can be observed that the simulated product yields match reasonably well with the experimental yields except for a few incongruities at lower and higher temperatures. Fig. 3 shows a good match between the model and experiments for the conversion of phenol, while the yields of benzene are overpredicted by the model at 400, 450 and 500 °C. It can be speculated that benzene acts as a precursor for the formation of char especially at high temperatures, which is not considered in the proposed reaction mechanism. It is worthwhile to mention that the product yields from the model correspond to a reaction time of 500–1000 ms. Typically, the time required decreased with increase in temperature.
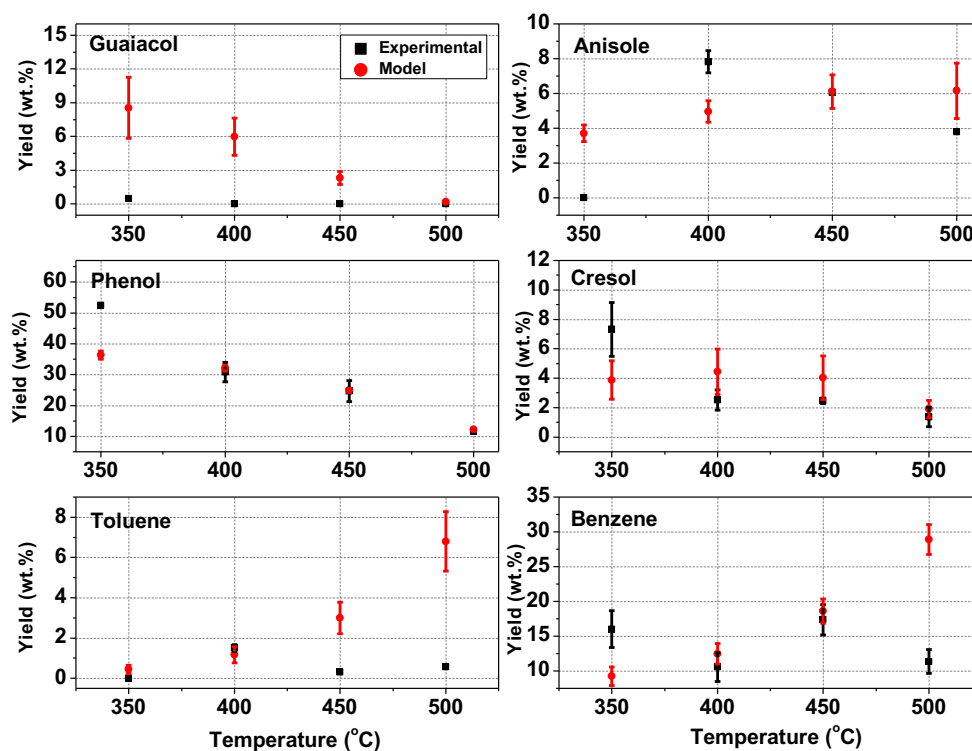
Fig. 5. Comparison of experimental and model yields of major products from catalytic HDO of syringol at different temperatures.

In the case of HDO of guaiacol, the trends of product yields at different temperatures are well captured by the model. Similarly, in the case of HDO of syringol, the trends of anisole, phenol and cresol are reasonably captured. In general, the model overpredicts the yields of few species, especially benzene and toluene, at high temperatures, which can be attributed, at least partially, to the low amount of carbon mass balance at high temperatures (Fig. 1). In addition to coke formation on the catalyst surface, gaseous carbon, in the form of CO, CO_2 and CH_4, is undetected in the GC/MS. The simulated yields of water are in the range of 2–19 wt%, 0.5–11.8 wt%, 3.3–10 wt% from phenol, guaiacol and syringol, respectively. The simulated yields of methanol are in the range of 6–20 and 37–38 wt% from guaiacol and syringol, respectively.

Through this study, a mechanistic modeling framework is proposed for the HDO of phenolic bio-oil compounds over H-ZSM-5 catalyst, and the model is validated using the product composition data collected in a Pyroprobe® analytical reactor. The rate parameters reported in this study serve as reasonable estimates, and there is a good scope to improve them by closing the carbon mass balance, and also by including kinetic rate information from quantum chemical density functional theory calculations performed on specific model compounds over the catalyst active site.

Declaration of Competing Interest

It is declared that the authors have no conflicts of interest or personal relationships that could have appeared to influence the work reported in this paper.

References

[1] M.S. Zanuttini, B.O.D. Costa, C.A. Querini, M.A. Peralta, Hydrodeoxygenation of m-cresol with Pt supported over mild acid materials, Appl. Catal. A: Gen. 482 (2014) 352–361.

[2] X. Zhu, L.L. Lobban, R.G. Mallinson, D.E. Resasco, Bifunctional transalkylation and hydrodeoxygenation of anisole over a Pt/HBeta catalyst, J. Catal. 281 (2011) 21–29.

[3] C.R. Lee, J.S. Yoon, Y.W. Suh, J.W. Choi, J.M. Ha, D.J. Suh, Y.K. Park, Catalytic roles of metals and supports on hydrodeoxygenation of lignin monomer guaiacol, Catal. Commun. 17 (2012) 54–58.

[4] A. Gutierrez, R.K. Kaila, M.L. Honkela, R. Slioor, A.O.I. Krause, Hydrodeoxygenation of guaiacol on noble metal catalysts, Catal. Today 147 (2009) 239–246.

[5] A.L. Jongerius, R.W. Gosselink, J. Dijkstra, J.H. Bitter, P.C.A. Bruijnincx, B.M. Weckhuysen, Carbon nanofiber supported transition-metal carbide catalysts for the hydrodeoxygenation of guaiacol, ChemCatChem 5 (2013) 2964–2972.

[6] T.S. Nguyen, S. He, L. Lefferts, G. Brem, K. Seshan, Study on the catalytic conversion of lignin-derived components in pyrolysis vapour using model component, Catal. Today 259 (2016) 381–387.

[7] M. Hellinger, H.W.P. Carvalho, S. Baier, D. Wang, W. Kleist, J.D. Grunwaldt, Catalytic hydrodeoxygenation of guaiacol over platinum supported on metal oxides and zeolites, Appl. Catal. A: Gen. 490 (2015) 181–192.

[8] W. Zhang, J. Chen, R. Liu, S. Wang, L. Chen, K. Li, Hydrodeoxygenation of lignin-derived phenolic monomers and dimers to alkane fuels over bifunctional zeolite-supported metal catalysts, ACS Sustain. Chem. Eng. 2 (2014) 683–691.

[9] C. Zhao, J.A. Lercher, Upgrading pyrolysis oil over Ni/HZSM-5 by cascade reactions, Angew. Chem. Int. (24) (2012) 5935–5940.

[10] D.Y. Hong, S.J. Miller, P.K. Agrawal, C.W. Jones, Hydrodeoxygenation and coupling of aqueous phenolics over bifunctional zeolite-supported metal catalysts, ChemComm 46 (2010) 1038–1040.

[11] C. Zhao, D.M. Camaioni, J.A. Lercher, Selective catalytic hydroalkylation and deoxygenation of substituted phenols to bicycloalkanes, J. Catal. 288 (2012) 92–103.

[12] J. Liu, M. Xiang, D. Wu, Enhanced phenol hydrodeoxygenation over a Ni catalyst supported on a mixed Mesoporous ZSM-5 zeolite and Al2O3, Catal, Letters 147 (2017) 2498–2507.

[13] D.K. Ojha, R. Vinu, Resource recovery via catalytic fast pyrolysis of polystyrene using zeolites, J. Anal. Appl. Pyrol. 113 (2015) 349–359.

[14] Z. He, X. Wang, Hydrodeoxygenation of model compounds and catalytic systems for pyrolysis bio-oils upgrading, Catal. Sustain. Energy 1 (2013) 28–52.

[15] M. Pelucchi, C. Cavallotti, A. Cuoci, T. Faravelli, A. Frassoldati, E. Ranzi, Detailed kinetics of substituted phenolic species in pyrolysis bio-oils, React. Chem. Eng. 4 (2019) 490–506.

[16] M. Saidi, F. Samimi, D. Karimipourfard, T. Nimmanwudipong, B.C. Gates, M.R. Rahimpour, Upgrading of lignin-derived bio-oils by catalytic hydro-deoxygenation, Energy Environ. Sci. 7 (2014) 103–129.

[17] D.P. Gamliel, G.M. Bollas, J.A. Valla, Two-stage catalytic fast hydropyrolysis of biomass for the production of drop-in biofuel, Fuel 216 (2018) 160–170.

[18] A.I. Vuori, J.B. Bredenberg, Thermal chemistry pathways of substituted anisoles, Ind. Eng. Chem. Res. 26 (1987) 359–365.

[19] N.T.T. Tran, Y. Uemura, A. Ramli, Hydrodeoxygenation of guaiacol over Al-MCM-41 supported metal catalysts: a comparative study of co and Ni, Process. Eng. 148 (2016) 1252–1258.

[20] T. Nimmanwudipong, R.C. Runnebaum, D.E. Block, B.C. Gates, Catalytic conversion of guaiacol catalyzed by platinum supported on alumina: reaction network including hydrodeoxygenation reactions, Energy Fuel 25 (2011) 3417–3427.